

Hydrogen Plasma-Based Reduction of Metal Oxides



Halvor Dalaker and Even Wilberg Hovig

Abstract Hydrogen is a candidate to replace carbon in metal production, as it can reduce some metal ores (e.g., iron ore). However, for other oxides, such as those of manganese and chromium, the situation is much more challenging. As the exotic species found in hydrogen plasma are much more reactive than molecular hydrogen, the use of hydrogen plasma can improve hydrogen reduction for all these oxides. Here, using a plasma arc melter, samples of Fe_2O_3 , Cr_2O_3 and MnO have been exposed to hydrogen plasma. Reactions between oxides and hydrogen have been observed in all cases, producing metallic iron, chromium, and manganese, hinting that plasma technology can play a part in sustainable metal production, allowing for carbon free production of chromium and manganese. The paper also discusses possible reaction mechanisms.

Keywords Hydrogen · Plasma · Manganese · Chromium · Steel · Sustainability

Introduction

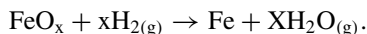
The metallurgical sector contributes to climate change through substantial CO_2 emissions. Some of these emissions are related to electricity production and can be mitigated by a change to a more renewable energy mix. Others result from carbon acting as a reducing agent in converting oxides to metal, with CO_2 as an unavoidable by-product. Sustainability therefore requires some combination of [1]:

- CO_2 -capture and storage
- The use of CO_2 -neutral biogenic carbon
- An entirely different and carbon free process, for example electrowinning.

H. Dalaker (✉)
SINTEF, Trondheim, Norway
e-mail: halvor.dalaker@sintef.no

E. W. Hovig
SINTEF, Oslo, Norway

Hydrogen is thought by many (e.g. [2]) to play a big role in decarbonising the metallurgical sector, as it can replace carbon in the reduction of some metal oxides, for example iron:

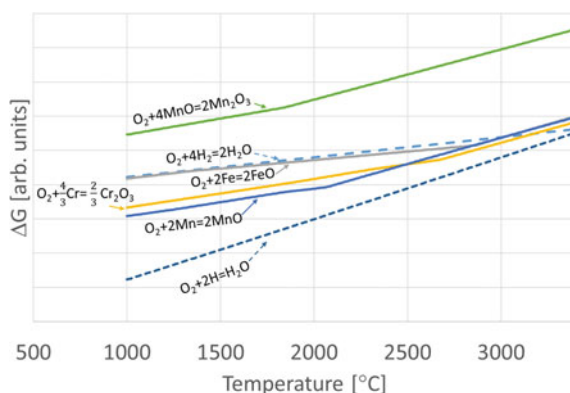


Some metal oxides, however, are too stable to be reduced by gaseous molecular hydrogen under normal conditions. Exciting the hydrogen to the plasma state will convert some of the molecular hydrogen into exotic species—such as monoatomic hydrogen, H, rotationally excited hydrogen, H_2^* , and ions such as H_2^+ and H^+ —that are more reactive towards metal oxides [3]. These species have the potential to react with metal oxides under conditions where molecular hydrogen would not [3], so if the reactive power of these species can be utilized, hydrogen-based extractive metallurgy of many more metals would become possible.

This is illustrated in Fig. 1, which shows an Ellingham diagram calculated using Factsage [4]. Each line shows the ΔG for the reaction between different elements and oxygen as a function of temperature. The relative position of these lines corresponds to the relative stability of the different oxides. The uppermost dashed line represents the reaction between hydrogen and oxygen to form water, while the very top line represents the reaction between MnO and oxygen to form Mn_2O_3 . Since the curve for the reaction $\text{O}_2 + 4\text{MnO} = 2\text{Mn}_2\text{O}_3$ lies above that of the reaction $\text{O}_2 + 2\text{H}_2 = \text{H}_2\text{O}$, hydrogen can be used in prereluction of higher order manganese oxides to MnO. Indeed, prereluction of manganese using hydrogen has received some attention [5, 6]. The reaction between metallic manganese and oxygen however, $\text{O}_2 + 2\text{Mn} = 2\text{MnO}$, lies below the hydrogen line, and reduction of MnO to metallic manganese by molecular hydrogen is thermodynamically unfavourable. The authors are not aware of any reports that metallic manganese has been produced from MnO with hydrogen.

The situation is similar for the chrome/chrome-oxide system, in that the Cr_2O_3 is more stable than H_2O across most relevant temperatures. However, at temperatures below approximately 2500 °C, Cr_2O_3 is less stable than MnO, and metallization

Fig. 1 Ellingham diagram for selected metal oxides, molecular hydrogen, and monoatomic hydrogen



of chromium during treatment of chromite ore with molecular hydrogen has been reported in the literature, albeit at very low levels [7].

In Fig. 1, the very lowest curve included is that for the reaction between oxygen and monoatomic hydrogen. It lies below all the other included curves for all temperatures below 3500 °C (At even higher temperatures, H₂O and H₂ both start to become unstable, so the study of reactions involving either specie as a reactant or product becomes less relevant). Monoatomic hydrogen then, should be able to reduce both chromium and manganese oxides to the metallic state. The plasma would also include charged species like H⁺ that are even more reactive [3], so the reactivity of the hydrogen plasma would be even greater than indicated by Fig. 1 that only considers H.

The situation of iron is slightly different since iron oxides can be reduced to metallic iron by molecular hydrogen. Indeed, hydrogen-based steelmaking is being explored by several players, including large steel producers [8, 9]. The argument for the study of hydrogen plasma in iron production is thus not based on *enabling* hydrogen use, but rather on *improvement*: it has been reported that the reduction rate of iron oxide using hydrogen in the plasma state is greater than that of the molecular state [10].

SINTEF have launched the HyPla project to investigate these opportunities [11]. The challenging physical conditions involved means that experimental investigations of plasma metallurgy are not straightforward, and a dedicated experimental rig is being built.

Filho et al. [12] reported on a method employing a plasma arc melter/suction caster to expose metal oxides to hydrogen plasma and to study the reduction of hematite. In this work we employ a similar method and apparatus to investigate the interaction between hydrogen plasma and Fe₂O₃, Cr₂O₃, and MnO.

Experimental Procedure

The oxides, in powder form, are cyclically exposed to hydrogen plasma in an Arc Melter AM200 (Edmund Bühler GmbH). An electric arc is struck between a tungsten electrode and a copper crucible, which generates a plasma plume extending out from the electrode. Prior to ignition, the process chamber is evacuated by a vacuum pump and then flushed with a gas mixture of 15% H₂ in Ar. During plasma exposure, the pressure in the processing chamber is held at a slight vacuum gauge pressure of 700 mbar. The position of the electrode is controlled by the operator and a distance between the tip of the electrode and the oxides is approximately 15 ± 5 mm. A schematic of the arc melter setup is shown in Fig. 2.

The experiments presented herein represent the early steps of method development. This means that exposure times and applied currents could not always adhere to a predetermined experimental plan but had to be adapted dynamically. In experiments with hematite, the initial aim was to do 60 s exposure times, but gas formation and foaming in some trials led to a violent reaction and failed experiments. Therefore,

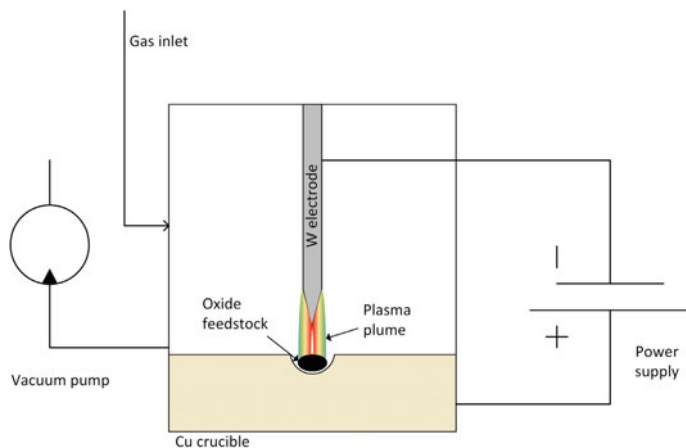


Fig. 2 Schematic of the experimental setup

in later tests, exposure was discontinued as soon as visual observations indicated gas formation.

The experiments with MnO and Cr_2O_3 were done together in a series with four samples, only two of which are reported here. In each cycle, all four samples were sequentially exposed for 30 s each between each evacuation and refill of the furnace chamber. With each cycle, a different sample was the first to be exposed to the plasma arc, to even out how much unreacted hydrogen each sample was exposed to. Also in these experiments, the applied current started out at 30A to avoid higher currents ejecting the powders from the crucible. Once the samples had melted together this was no longer an issue, and the current could gradually be increased over several cycles to 100A. The complete overview of exposure times, current, and gas replenishing intervals are given in Table 1.

The samples were analysed using Electron beam Micro Probe Analyser (EPMA), both for imaging and for use of Electron Diffraction (EDS) for chemical analysis.

Results and Discussion

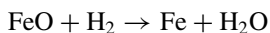
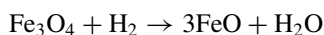
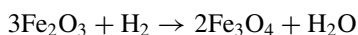
General Observations

As mentioned in the experimental description, during experiments with hematite there was considerable gas evolution, which caused the samples to expand. A possible explanation is that this was caused by water vapour forming from the reaction of hematite. However, in all potential reactions, the amount of product H_2O is the same as the reactant H_2 (the situation will be the same if 2H is considered instead of H_2):

Table 1 Overview of experiments

| Sample | Fe ₂ O ₃ | | MnO | | | Cr ₂ O ₃ | | |
|--------|--------------------------------|----------|-------------|----------|-------------------------|--------------------------------|----------|-------------------------|
| | Current [A] | Time [s] | Current [A] | Time [s] | Exposed as x/4 in cycle | Current [A] | Time [s] | Exposed as x/4 in cycle |
| 1 | 45 | 60 | 30 | 30 | 1 | 30 | 30 | 3 |
| 2 | 45 | 24 | 30 | 30 | 4 | 30 | 30 | 2 |
| 3 | 45 | 16 | 40 | 30 | 3 | 40 | 30 | 1 |
| 4 | 45 | 21 | 50 | 30 | 2 | 50 | 30 | 4 |
| | H ₂ replenished | | | | | | | |
| 5 | 45 | 25 | 60 | 30 | 1 | 60 | 30 | 3 |
| 6 | 45 | 13 | 70 | 30 | 4 | 70 | 30 | 2 |
| 7 | 45 | 30 | 70 | 30 | 3 | 70 | 30 | 1 |
| | H ₂ replenished | | | | | | | |
| 8 | 45 | 19 | 80 | 30 | 2 | 80 | 30 | 4 |
| 9 | 45 | 30 | 80 | 30 | 1 | 80 | 30 | 3 |
| 10 | 45 | 30 | 100 | 30 | 4 | 100 | 30 | 2 |
| 11 | – | – | 100 | 30 | 3 | 100 | 30 | 1 |
| 12 | – | – | 100 | 30 | 2 | 100 | 30 | 4 |

During experiments with MnO and Cr₂O₃, the hydrogen was replenished after each cycle. For experiments with Fe₂O₃, hydrogen was replenished after cycle 4 and cycle 7, as indicated in the table



In other words, gas volume expansion as a result of the chemical reaction does not appear to be a viable explanation.

The cooling effect of the water-cooled copper substrate is substantial compared to the thermal mass of the small samples. It is therefore possible that evolved H₂O gas trapped inside the sample could condense once the arc is turned off. During re-heat, these water droplets could boil and expand, but the issue remains unresolved.

When the chamber is vented after each cycle, the pressure drops from 700 mbar to 0.05 mbar. In experiments with hematite, at this point a cloud of mist or dust becomes visible, and the viewport of the instrument fogs over. This could perhaps be water vapour resulting from a reaction between hydrogen and oxide, or solid dust being blown away from surfaces by the moving gases. In experiments with Cr₂O₃ and MnO, the same phenomena appears but to a much lower degree. During exposure,

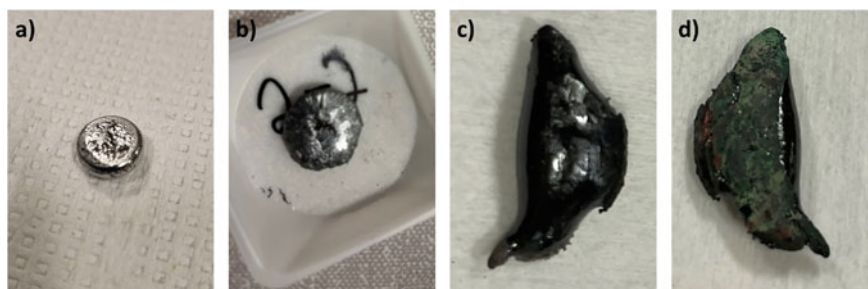


Fig. 3 Photographs of samples after exposure to hydrogen plasma. The initial material in each figure is respectively: **a** Fe₂O₃, **b** Cr₂O₃, **c** and **d** MnO

when in contact with the Cr₂O₃ sample the plasma plume had hues of green, yellow, and orange, while when in contact with the MnO sample the arc was bluish.

For experiments with both Cr₂O₃ and MnO, there was considerable loss of material. This may be because of the volatility of both Cr and Mn at the high temperatures. Dust/condensate was found around the samples at the end of experiments, but these were not analysed at this stage.

Figure 3 shows images of the samples after hydrogen plasma exposure of: Fe₂O₃ (a), Cr₂O₃ (b), and MnO (c and d). The Fe₂O₃ sample appeared metallic to the eye. The bottom face, towards the copper substrate during experiments, was quite shiny, while the top surface that faced out towards the interior of the arc melter, was duller. The sample was magnetic: the bottom surface strongly magnetic, and the top surface weakly magnetic.

The Cr₂O₃ and MnO samples showed an even greater contrast between the top and bottom faces. Figure 3c shows the top surface of the MnO sample as being shiny while the bottom (3d) is rock-like.

EPMA Analysis and Thermodynamic Considerations

In this section, the EPMA images of the samples are presented, and the observed phases are discussed. In terms of thermodynamics, FactSage has been used with the FactOxide and FSstel databases [4].

Figure 4a shows the EPMA-image of a part of the Fe₂O₃-sample after exposure to hydrogen plasma. EDS analyses were taken in several spots in the sample. The bright phase was determined to be metallic iron by EDS. While the quantification of chemical composition by EDS is somewhat uncertain, an average of 5 measurements in the oxide phase gave an O:Fe mass ratio of 2.63, corresponding to a molar ratio of 1.33. This is consistent with magnetite, Fe₃O₄, which matches the observation of magnetism of the sample. The light phase contains only iron, as confirmed by EDS. No difference in the chemical composition of the oxide phase could be detected

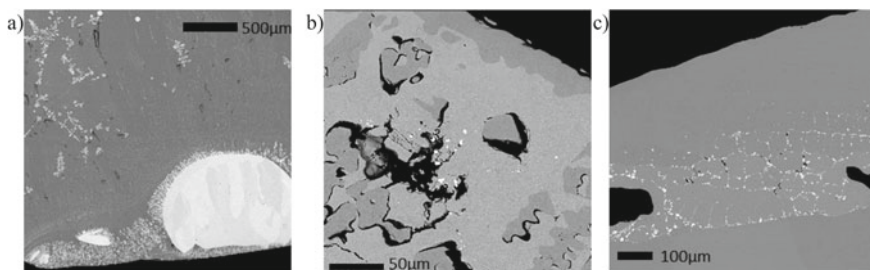


Fig. 4 EPMA images of samples after exposure to hydrogen plasma. The initial material in each figure is respectively: **a** Fe_2O_3 , **b** Cr_2O_3 , **c** MnO . Note the differences in magnification

between the top and the bottom of the sample, and the sample thus appears to consist mainly of magnetite, with droplets of metallic iron inclusions. The observation that the bottom of the sample is more magnetic than the top is not due to a difference in oxide phases, but rather because more of the metallic phase is found at the bottom of the sample. It would be expected that iron would more easily be formed at the top of the sample, where it is exposed to hydrogen plasma and high temperatures, but gravitational separation could cause the denser metal to collect at the bottom of the sample.

Figure 4b shows the EPMA image of the Cr_2O_3 sample. Two different oxide phases and a metallic phase are identified using EDS. The darkest phase is consistent with Cr_2O_3 , while the lighter oxide phase has a Cr:O ratio that corresponds to CrO. The metallic phase is measured at more than 90 wt.% Cr, with an average of 2.5 wt.% Fe 2.3 wt.% Cu and 1.3 wt.% O. It must again be stressed that the measured quantities should not be taken as more than an indication, but this signal is consistent with a metallic phase that is mostly chromium. The oxygen signal can be due to surrounding oxides, the copper can come from the substrate, while the iron is a plausible impurity in the Cr_2O_3 starting material (99.6% pure, no other information on impurities given). In other words, metallic chromium has been formed.

CrO is not thermodynamically stable as a solid, but it exists in liquid form at high temperatures. When considering only pure substances, liquid Cr_2O_3 decomposes into liquid CrO and solid CrO_2 at temperatures above 2690 °C. If liquid CrO cools without interacting with CrO_2 (for example due to rapid quenching), it should solidify as equal amounts of Cr and Cr_2O_3 at equilibrium.

Some possible explanations for the existence of metallic chromium, the merits of which will be discussed in the following, are:

- (A) Cr forms as CrO cools and separates into Cr_2O_3 and Cr, the CrO having been formed from thermal decomposition of Cr_2O_3 into CrO and CrO_2 .
- (B) Cr forms as CrO cools and separates into Cr_2O_3 and Cr, the CrO having been formed from the reduction of Cr_2O_3 by H_2 or H.
- (C) Cr is formed by the reduction of Cr_2O_3 by H_2 or H. First to CrO, and then some CrO is further reduced into Cr.

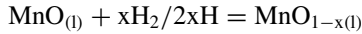
The lack of any CrO_2 is a strike against explanation A, although CrO_2 could behave differently to CrO during cooling and reach equilibrium during cooling. Further, the formation of Cr and Cr_2O_3 during the solidification of CrO would give Cr as a solid (even with a few % of Fe), meaning that A and B fail to explain how the metallic phase was able to coalesce as the pearls seen in Fig. 4b.

Of the three explanations then, C remains viable. While reaction to metallic Cr by H_2 is not particularly favourable thermodynamically speaking ($\Delta G > 0$ for $T < 3173$ °C), it cannot be ruled out. Also, it remains undetermined whether reactions involving monoatomic hydrogen or other excited H-species have played a role.

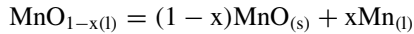
Figure 4c shows the MnO -sample after exposure to the plasma. The bright phase was confirmed to be metallic manganese. Interestingly, only a single oxide phase was detected, one that corresponds to MnO . In other words, the strikingly different surfaces seen in Fig. 3c, d are the same material. The shiny phase is only quite thin, maybe 100 μm , below which is a cellular structure with metallic manganese on the grain boundaries. The rest of the sample maintains its original chemical and visual characteristics.

If the metallic manganese existed as a liquid at high temperature, it can be imagined that the pattern has been caused by liquid manganese being pushed by the solidifying oxide until it collects in the gaps between the oxide zones.

The distribution of the manganese is reminiscent of precipitates formed at the grain boundaries of a cooling sample. In which case the high-temperature starting phase may have been an oxygen-depleted MnO -phase:



As this phase solidifies, metallic manganese could be expelled



However, we have found no mention in the literature of oxygen deficient liquid MnO .

Another explanation is that during exposure, liquid Mn exists on the surface of the sample, but as the plasma is turned off and the temperature starts dropping it will to some extent react with H_2O to re-form MnO at the top of the sample most exposed to the H_2O -containing atmosphere. Some metallic manganese below the surface could remain unreacted between a protective layer of MnO , but this does not adequately explain the formation of the observed microstructure. Thus, the exact mechanism remains unconfirmed, but it seems most likely that metallic Mn has been pushed by solidifying MnO , perhaps in a combination of reactions between H_2O and Mn .

Filho et al. [12] presented images of partially converted samples that showed that over the course of 30 1-min cycles the hematite sample transformed first into magnetite and then into metallic iron. Compared to those results, our Fe_3O_4 sample shows less conversion than the one they present as having been exposed to five cycles. This indicates that with an increased number of cycles, eventual full conversion to metallic iron could be possible in our setup, although electrical parameters also

differ (800A vs. 45A). This in turn suggests that increased amounts of metallic manganese and chromium could also be obtained with increased numbers of cycles and/or increased currents. In our setup we have experienced considerable electrode wear at higher currents, so substantial changes to the setup might be necessary. It must also be noted that there is a limit to how many cycles the samples can effectively be exposed to, as the material is lost as vapour and/or dust during exposure to plasma. Furthermore, as was already mentioned, back-reactions with H_2O may also occur.

However, it is important to note that these challenges are mostly related to the experimental method. The main message of the current work is that Cr_2O_3 and MnO have been exposed to hydrogen plasma at high temperatures, successfully obtaining metallic products completely without carbonaceous reductants. Of course, these are early days and a lot of work remains, for example in avoiding the produced metals to be re-oxidised by the water vapour. But if these results can eventually be reproduced and improved in an industrial setting, it can be a significant step forward for sustainable metal production. If this happens it will likely be in conditions not directly comparable to those obtained in a plasma arc melter. Other experimental setups will likely be necessary for the process development.

Conclusions

Using a plasma arc melter, samples of Fe_2O_3 , MnO and Cr_2O_3 have been exposed to hydrogen plasma, producing metallic Fe, Mn, and Cr.

The Fe_2O_3 sample was converted to Fe_3O_4 with significant amounts of metal droplets. In the Cr_2O_3 and MnO samples much less metal was found than in the Fe_2O_3 sample, and in the Cr_2O_3 sample the metastable phase CrO was found in significant amounts.

The mechanisms for Cr and Mn formation remain unclear, even though it is suspected that plasma radicals such as monoatomic hydrogen have played a role.

Comparisons with similar work suggest that iron conversion could be increased by increased current and/or exposure time, while it is less certain how well this approach would work for Cr_2O_3 and MnO due to increased material loss.

References

1. Kero IT, Dalaker Halvor, Osen KS, Ringdalen E (2021) Some carbon-free technologies for manganese ferroalloy production. In: Proceedings of the 16th international ferro-alloys congress (INFACON XVI). Available at SSRN: <https://ssrn.com/abstract=3926069> or <https://doi.org/10.2139/ssrn.3926069>
2. European Commission (2020) Communication from the commission to the European parliament. The Council, The European economic and social committee and the committee of the regions—a hydrogen strategy for a climate-neutral Europe. https://ec.europa.eu/energy/sites/ener/files/hydrogen_strategy.pdf

3. Sabat KC, Rajput P, Paramguru RK, Bhoi B, Mishra BK (2014) Reduction of oxide minerals by hydrogen plasma: an overview. *Plasma Chem Plasma Process* 34:1–23. <https://doi.org/10.1007/s11090-013-9484-2>
4. Bale CW, B elisle E, Chartrand P, Deckerov SA, Eriksson G, Gheribi AE, Hack K, Jung IH, Kang YB, Melan on J, Pelton AD, Petersen S, Robelin C, Sangster J, Van Ende MA (2016) FactSage thermochemical software and databases, 2010–2016. *Calphad* 54:35–53. www.factsage.com
5. Barner HE, Mantell CL (1968) Kinetics of hydrogen reduction of manganese dioxide. *Ind Eng Chem Process Des Dev* 7(2):285–294. <https://doi.org/10.1021/i260026a023>
6. Safarian J (2022) A sustainable process to produce manganese and its alloys through hydrogen and aluminothermic reduction. *Processes* 10(1):27. <https://doi.org/10.3390/pr10010027>
7. Davies J, Paktunc D, Ramos-Hernandez J, Tangstad M, Ringdalen E, Beukes J, Bessarabov D, du Preez S (2022) The use of hydrogen as a potential reductant in the chromite smelting industry. *Minerals* 12:534. <https://doi.org/10.3390/min12050534>
8. SSAB (2021) The world’s first fossil-free steel ready for delivery. <https://www.ssab.com/en/news/2021/08/the-worlds-first-fossilfree-steel-ready-for-delivery> [Accessed 03 Aug 2022]
9. Thyssenkrupp (2021) Green hydrogen for the decarbonization of the steel industry: Thyssenkrupp Steel and STEAG agree on hydrogen supply. <https://www.thyssenkrupp-steel.com/en/newsroom/press-releases/thyssenkrupp-steel-and-steag-agree-on-hydrogen-supply.html> [Accessed 03 Aug 2022]
10. Sefteljani MN, Schenk J (2018) Thermodynamic of liquid iron ore reduction by hydrogen thermal plasma. *Metals* 8(12):1051. <https://doi.org/10.3390/met8121051>
11. SINTEF (2021) HyPla-Hydrogen plasma for CO₂-free metal production. <https://www.sintef.no/en/projects/2020/hypla-hydrogen-plasma-for-co2-free-metal-production/> [Accessed 03 Aug 2022]
12. Souza Filho IR, Ma Y, Kulse M, Ponge D, Gault B, Springer H, Raabe D (2021) Sustainable steel through hydrogen plasma reduction of iron ore: process, kinetics, microstructure, chemistry. *Acta Mater* 213:116971. <https://doi.org/10.1016/j.actamat.2021.116971>